Mon. Not. R. Astron. Soc. **287,** 199–210 (1997)

Radio and extreme-ultraviolet observations of CF Tucanae

A. G. Gunn,[1]★ V. Migenes,[2]† J. G. Doyle,[1] R. E. Spencer[3] and M. Mathioudakis[4]
[1]*Armagh Observatory, College Hill, Armagh BT61 9DG*
[2]*ATNF, PO Box 76, Epping, NSW 2121, Australia*
[3]*NRAL, Jodrell Bank, Lower Withington, Cheshire SK11 9DG*
[4]*Department of Pure & Applied Physics, Queen's University of Belfast, Belfast BT7 1NN*

Accepted 1996 December 30. Received 1996 December 16; in original form 1996 November 11

ABSTRACT

We present contemporaneous EUV and radio observations obtained for the totally eclipsing chromospherically active RS CVn-type binary CF Tucanae. Observations were made with the ATNF Compact Array at 6 and 3.6 cm over one complete orbital cycle of the system, and with the *EUVE* Deep Survey/Spectrometer telescope over five orbital cycles. We obtained a strong detection of the source (1.9 mJy at 6 cm and 1.1 mJy at 3.6 cm) in the radio. Both EUV and radio flux levels appear to show a clear modulation at the orbital period with a maximum at phase 0.5 which indicates the existence of an intra-binary region of activity. This has important consequences for the details of coronal formation and field interaction in active close binary stars. We interpret the EUV emission as an isotropically radiating thermal source; on the other hand, the radio emission shows evidence of intrinsic gyromagnetic directivity. We also demonstrate that contemporaneous EUV and radio observations are not sufficient to determine the characteristics of the gyro-emission electron population.

Key words: stars: activity – binaries: close – stars: flare – stars: late-type – stars: variables: other – radio continuum: stars.

1 INTRODUCTION

Radio emission from active binary stars has now been observed for over 20 years, but in that time only tentative suggestions have been made on the relationship with underlying coronal and chromospheric activity. Relatively high radio fluxes are a common feature in RS CVn systems (Drake, Simon & Linsky 1989) and Algol-type binaries (Umana et al. 1993). The characteristics of the radio emission are similar to those found in highly active single stars (e.g. dMe stars). A non-thermal gyrosynchrotron emission process from mildly relativistic electrons in coronal magnetic fields is usually invoked to explain the activity. The level of activity in late-type stars is believed to be a manifestation of the strong dynamo-generated magnetic fields, and correlation between activity and rotation supports this contention (Stewart et al. 1988; Gunn 1996).

There has been some debate about the relationship between the radio and X-ray regimes. Güdel & Benz (1993) found $L_X \sim 10^{15.5} L_R$ valid over six orders of magnitude in both variables for all active late-type stars and solar flares. This correlation may be explained if it is assumed that the same population of electrons is responsible for the X-ray and radio emission, and may also imply a possible spatial link between the X-ray- and radio-emitting regions. However, the X-ray emission is consistent only with a population of *thermal* electrons with characteristic temperatures of 10^7 K, whereas the radio emission seems to require a *non-thermal* population.

For RS CVn stars it is often found that radio emission associated with flare events arises in regions smaller than or comparable to a stellar radius, while the quiescent emission arises from an extended halo whose dimensions are comparable to the overall size of the binary system. Very long baseline interferometry (VLBI) observations by Mutel et al. (1985) have also indicated the extensive nature of radio coronae. These authors propose a time-dependent model of the emission to account for the core–halo morphology. Electrons are accelerated in a compact region with strong magnetic fields which is initially optically thick and produces a positive spectral index α ($S \propto \nu^{\alpha}$) and a low degree of circular polarization. As the source expands radially, the magnetic field decreases and the electrons radiate by synchrotron processes. Eventually the source expands enough to become optically thin and appears as an extended halo with a negative spectral index and a high degree of circular polarization. Such a model is consistent with the evolution of magnetic loops on the Sun. For Algol-type binaries the radio coronae are also observed to be very extensive and the core–halo model also seems to account for their observed properties.

An alternative explanation of the extensive nature of radio coronae around RS CVn binaries is that provided by Uchida &

★Present address: NRAL, Jodrell Bank, Lower Withington, Cheshire SK11 9DG.
†Present address: VSOP Project, National Astronomical Observatory, Osawa 2-21-1, Mitaka, Tokyo 181, Japan.

Sakurai (1983). The existence of differential rotation can lead to twisting of magnetic flux tubes, and the subsequent reconnection of loops can give rise to extended coronae enveloping both late-type stars in an RS CVn binary. Currently this interacting field model suffers from the observation of similar large-scale radio emission in some active single stars and Algol-type systems. Algols cannot be expected to possess an efficient field interaction mechanism, since the primary components have very inefficient dynamos. In Algol itself, Lestrade et al. (1988) clearly showed that the radio emission was associated only with the active K-type star in the system. However, Lestrade (1996) recently presented an analysis of VLBI astrometry for two RS CVn stars, UX Ari and σ^2 CrB, which clearly showed the preferred site of the quiescent emission in the intra-binary region.

It is now recognized that the intensity of the active binary radio emission during quiescent (non-flaring) periods varies systematically during the binary orbit, and this has been used to investigate the radio magnetosphere at high resolution by eclipse mapping in addition to VLBI techniques. However, the intrinsic or geometric nature of these variations is somewhat unclear. Brown, Broderick & Neff (1979) presented Very Large Array (VLA) observations of the RS CVn system AR Lac, but could not determine whether phase-correlated flux variations were related to eclipses or to rotational modulation of stellar active regions. Doiron & Mutel (1984) also observed clear flux variations on AR Lac at both 2 and 20 cm, but these could not be associated with the eclipse cycle and were probably intrinsic to the source (i.e. flaring or directed emission). However, the possibility of intrinsic directivity of radio emission has not been considered in detail for active stars.

In this paper we present and discuss continuous interferometer observations obtained for CF Tucanae simultaneously at 6 and 3.6 cm over one complete orbital cycle of the system. We present radio images at both frequencies for this binary system and discuss the variation of the observed flux levels. A preliminary analysis of the radio data was presented by Gunn et al. (1996a). We have also analysed contemporaneous extreme-ultraviolet (EUV) data from the Deep Survey/Spectrometer telescope on board the *Extreme Ultraviolet Explorer* (*EUVE*). We compare the radio and EUV light curves, suggest possible scenarios for the active regions in the CF Tuc system and discuss the mechanisms of producing the observed fluxes. We draw particular attention to the inadequacy of contemporaneous EUV and radio observations in determining the characteristics of the gyrosynchrotron electron population, discuss the possibility of intrinsic directivity in stellar radio emission and suggest that radio emission may originate preferentially in the intra-binary region in close binary systems.

2 CF TUCANAE

CF Tucanae is an eclipsing RS CVn-type binary with an orbital period of 2.798 d, and consists of a G0 V primary and a K4 IV secondary of radii 1.67 and 3.32 $R_\odot$, respectively, with a separation of about 5.35 $R_\odot$. The system lies at a distance of about 54 pc (Collier et al. 1982) and has an orbital inclination of $\sim 71°$ (Collier, Hearnshaw & Austin 1981). Fig. 1 shows a schematic representation of the geometry of the system at both conjunctions and quadratures. Optical photometric analysis of CF Tuc has been provided by, amongst others, Cameron, Hearnshaw & Austin (1981), Rucinski (1983), Budding & McLaughlin (1987) and Budding & Zeilik (1995). Analysis of the Hδ and Ca II H and K lines by Cameron, Hearnshaw & Austin (1981) showed that Ca II emission originates solely on the cooler star in this system while the Hδ line is much stronger in the hotter star. These authors also analysed *BVRI* photometry which revealed a quasi-sinusoidal variation with twice the orbital frequency, implying that tidal distortion causes ellipticity of CF Tuc's components. This variation was in addition to the spot-wave distortion in the light curve. They concluded that the cool component in CF Tuc exhibits intense surface activity which is confined to a small region on one hemisphere. There has been no detailed spectroscopic study of CF Tuc, although Collier et al. (1982) observed filled-in absorption in the Hα line.

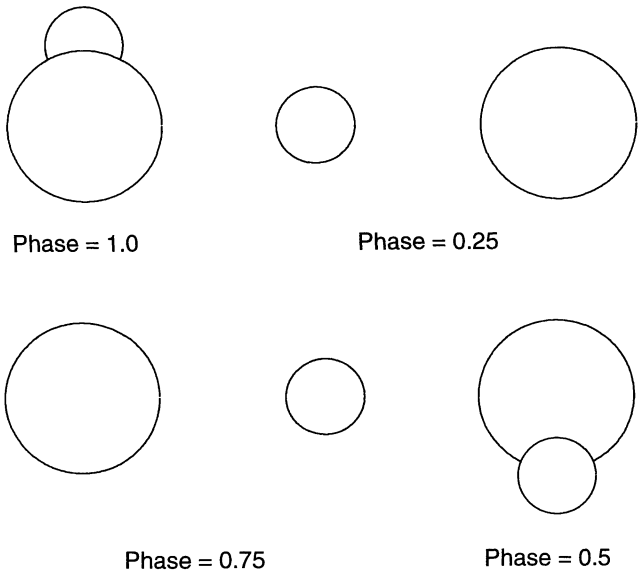

Figure 1. Schematic representation of the CF Tucanae system at both conjunctions and quadratures of the orbit. At primary conjunction (phase 1.0) the hotter G star is eclipsed by the cooler K component.

Numerous measurements of CF Tuc have been performed in the radio, X-ray and UV regions. Owen & Gibson (1978) failed to detect the system in their 6-cm survey. Also, Collier et al. (1982) could not detect CF Tuc above 10 mJy at 5 GHz during observations with the Parkes 64-m telescope. Slee et al. (1987) observed CF Tuc with the same instrument and measured the 5-GHz flux at 7.1 mJy. Dempsey et al. (1993) measured the X-ray flux at $L_X = 3.45 \times 10^{30}$ erg s^{-1} using *ROSAT* All Sky Survey data, while Drake, Simon & Linsky (1992) report a flux of 3.7×10^{30} erg s^{-1} based on a search of the *Einstein* IPC Slew Program data. Walter & Bowyer (1981) give an X-ray luminosity of 2.3×10^{30} erg s^{-1} based on their *Einstein* observations. Recently, Kürster & Schmitt (1996) presented *ROSAT* PSPC observations of a long-lived energetic flare on CF Tuc, whilst Schmitt et al. (1996) discussed EUV spectral observations of the system.

3 OBSERVATIONS AND DATA REDUCTION

3.1 ATCA observations

Observations were carried out with the 6-km Australia Telescope Compact Array (ATCA) located near Narrabri, NSW, and operated by the Australia Telescope National Facility (ATNF) for CSIRO. The ATCA consists of five 22-m antennas on a 3-km track together with an antenna located 6 km to the west. A recent description of the array can be found in Manchester (1991). Observations began at 00:36 UT on 1994 August 27 and lasted 72 h in order fully to investigate a complete orbital cycle of the binary (67.15 h). The

array was calibrated in amplitude by convenient observations of the primary flux calibrator 1934−638 assuming flux densities of 6.33 and 2.59 Jy at the wavelengths of 6 and 3.6 cm respectively. Phase calibration was achieved by observations of the compact source 2142−758 taken every 15–20 min. The target data consist of approximately 15-min scans of 15-s integrated amplitude and phase measurements. All observations were conducted simultaneously at two frequencies: 4.8 GHz (6 cm) and 8.64 GHz (3.6 cm) with instrumental bandwidths of 128 MHz. The effective bandwidth was approximately 84 MHz across 20 channels which were then averaged.

The data were processed using the software packages AIPS and MIRIAD. Inspection of the phase calibrator data and subsequent mapping showed that this was in fact a triple source at 6 cm but appeared to be point-like at 3.6 cm. Since the calibrator amplitude variations were less than 2 per cent due to the weakness of the secondary and tertiary components, no correction was performed to account for the assumption of a point source for the calibration. The induced flux errors due to this procedure are well below the noise level in the target.

Imaging of the target field revealed three point-like confusing sources with flux levels significantly above the noise. These were removed by fitting single 2D Gaussian profiles in the image plane and subtracting these models from the visibility data. Analysis of the final data set involved vector averaging the visibilities (taken at the phase centre) and plotting these against time. To achieve this the target position was accurately determined by fitting a 2D Gaussian model and then shifting the data to align the peak position with the phase centre. This allows the mapping procedure to be by-passed and the data sampled with the full temporal resolution of the array. However, we elected to average the visibilities over several scan lengths. The penalty of directly plotting visibilities is a poorer signal-to-noise ratio, and the different temporal weighting gives rise to small discrepancies between the map- and visibility-determined mean fluxes. As a check, however, we performed the mapping procedure for data segments of approximately 1-h duration (three scan lengths) and measured the resulting peak flux at the target position. The data segments used for the mapping were the same as those used to form the hourly vector-averaged components.

3.2 *EUVE* observations

CF Tuc was observed with the Deep Survey/Spectrometer telescope on board the *Extreme Ultraviolet Explorer* (*EUVE*) from approximately 02:30 on 1994 August 28 to 18:00 on September 7 with a total exposure time of 276 ks. The overlap of the *EUVE* observations with our radio observations prompted us to examine the EUV data. Here we will only concentrate on the Deep Survey (DS) data. Schmitt et al. (1996) have recently given a comprehensive analysis of the *EUVE* spectrum of CF Tuc recorded during these observations.

The DS instrument is a short-wavelength imaging system with a field of view of approximately 5°. In pointed mode the source lies

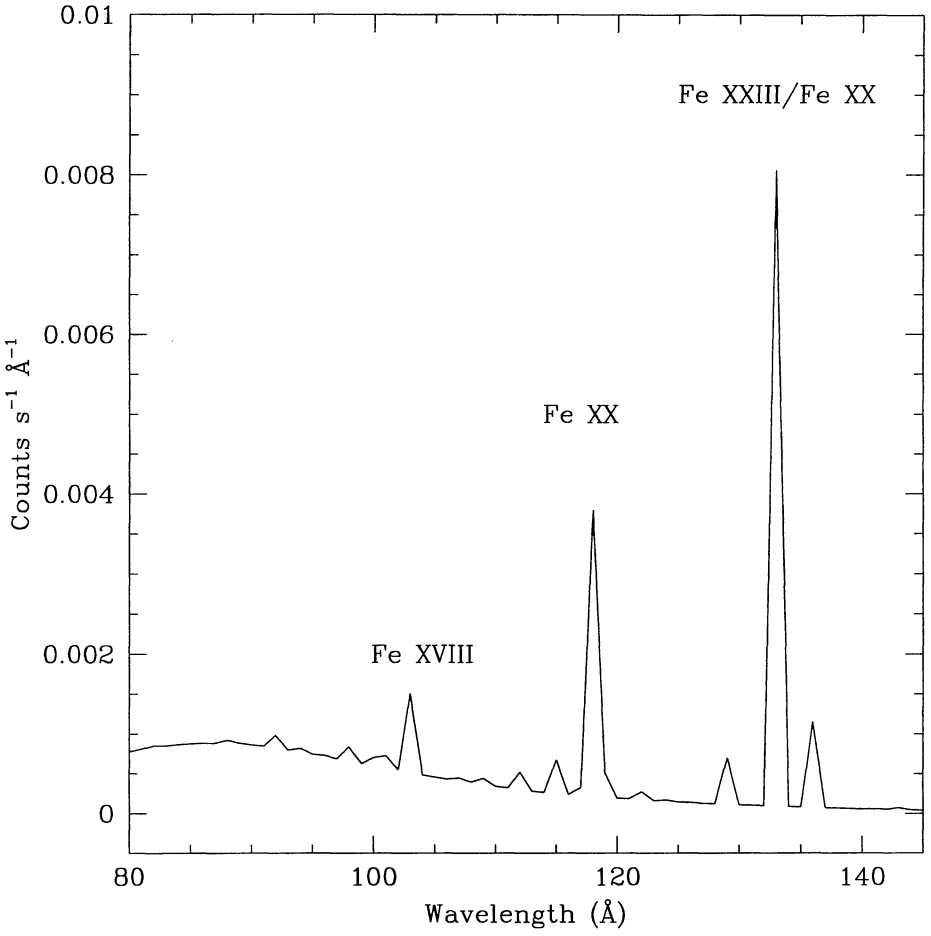

Figure 2. Model EUV spectrum of CF Tuc generated using the average count rate, a distance of 54 pc, log N_H = 19.2 cm^{-2}, He I/H I = 0.1 and log T = 7.2.

continuously on the Lexan/B section of the filter. The 10 per cent transmission bandpass of the DS Lex/B is 66–180 Å (0.069–0.187 keV) with a peak sensitivity of 28 cm^2 at 90 Å. Data were collected for approximately 30 min of the 90-min orbit of the *EUVE* satellite in this mode. For more details on the DS instrument the reader is referred to Malina et al. (1994) and Bowyer et al. (1994). Since CF Tuc is a relatively bright EUV source, it was easily identified on the DS detector. The *EUVE* data have been reduced with the latest version of the EUV software EGOCS 1.6 and EGODATA 1.11 (Miller & Abbott 1995). Further analysis of the data was performed using the PROS X-RAY tasks available in IRAF. The source region is defined by a circle with a radius large enough to encompass the instrument point-spread function, where the background is estimated in an annulus centred on the same position. The data were binned into 10 000-s time bins. Schmitt et al. (1996) used a different binning time for these data.

We have determined EUV fluxes from the count rates using the Mewe, Gronenschild & van den Oord (1985) line emissivities for an average coronal temperature of $\log T = 7.2$. The interstellar medium attenuation has been computed using the hydrogen and helium photoionization cross-sections compiled by Rumph, Bowyer & Vennes (1994). An interstellar hydrogen column density of $\log N_H = 19.2\,cm^{-2}$ and an He I/H I ratio of 0.1 were used in the calculation. Using the above parameters, this translates to a conversion factor of 1.07×10^{-13} erg cm^{-2} s^{-1} per count per ks. Taking the average mean count rate of 0.043 count s^{-1} we derive a mean observed flux of 4.6×10^{-12} erg cm^{-2} s^{-1} in the DS Lex/B band. At the assumed distance of 54 pc this corresponds to an EUV luminosity of 1.6×10^{30} erg s^{-1} which compares well with X-ray luminosities given by Dempsey et al. (1993), Walter & Bowyer (1981) and Drake et al. (1992). Note that the DS filter has a factor of two more in effective area than the all-sky survey data used by Mitrou et al. (1997).

Using the same parameters and emissivities as above and assuming a single-temperature coronal model of $\log T = 7.2$, we have generated an emission measure. This was then used to generate a model spectrum which was then folded through the *EUVE* DS effective area. The resulting model EUV spectrum for CF Tuc is shown in Fig. 2. In this spectrum coronal lines (due to Fe) contribute about 20 per cent of the flux, which compares well with the line-to-continuum ratio of 0.87 derived from the observed spectrum by Schmitt et al. (1996). We therefore assume that the continuum EUV flux from CF Tuc is about 80 per cent of the measured flux. Since the corona can assume a range of temperatures, this value is an upper limit.

4 RESULTS AND DISCUSSION

4.1 Radio images

Fig. 3 shows the restored image of CF Tuc at 6 cm. The AIPS task MX was used to obtain maps 512 × 512 pixels in size with a pixel size of 0.4 arcsec. The map shows an unresolved point source with a peak flux level of 1.91 mJy $beam^{-1}$. The angular extent of this source

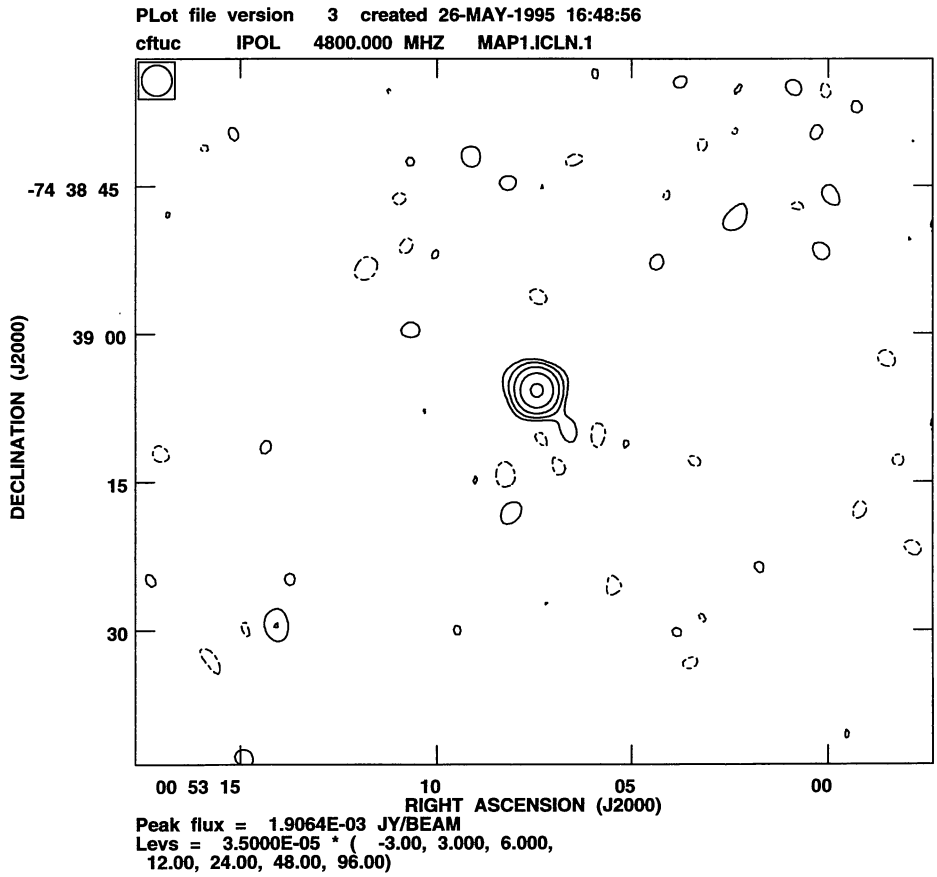

Figure 3. The ATCA radio map of the area around CF Tuc at 6 cm. The restoring beam is shown in the upper left-hand corner. Plotted flux levels are at −3, 3, 6, 12, 24, 48 and 96 times the rms noise level.

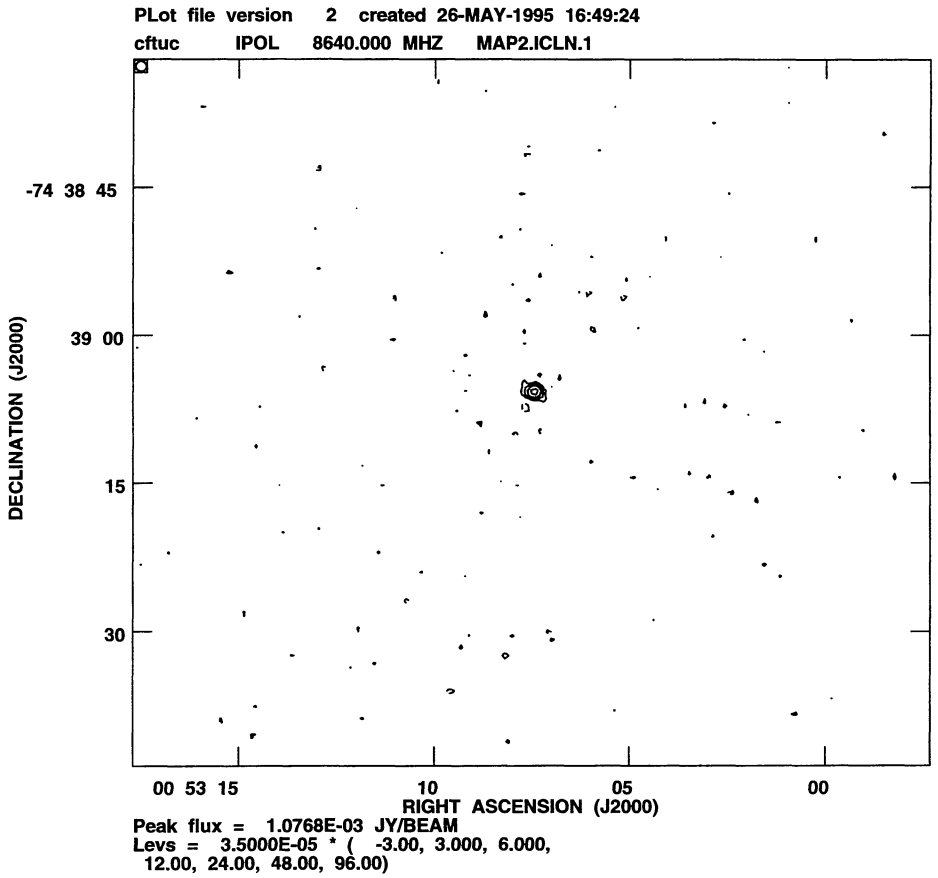

Figure 4. The ATCA radio map of the area around CF Tuc at 3.6 cm. The restoring beam is shown in the upper left-hand corner. Plotted flux levels are at −3, 3, 6, 12, 24, 48 and 96 times the rms noise level.

(< 1.0 arcsec) is comparable to the synthesized beam (2.0 arcsec). The maximum angular diameter of the CF Tuc system is ~0.9 mas. The mean J2000 position ($\alpha = +00^h\ 53^m\ 07\overset{s}{.}45$, $\delta = -74°\ 39'\ 05\overset{''}{.}73$) is consistent with the most accurate optical position allowing for proper motion. The measured rms noise level (5σ) in the image is 2×10^{-4} Jy beam^{-1}. Also in the field (but not displayed in Fig. 3) are three unresolved objects of peak flux levels 1.1, 0.2 and 0.7 mJy at positions $\alpha = 00^h\ 52^m\ 30^s$, $\delta = -74°\ 37'\ 48''$, $\alpha = 00^h\ 52^m\ 18^s$, $\delta = -74°\ 38'\ 10''$ and $\alpha = 00^h\ 53^m\ 38^s$, $\delta = -74°\ 35'\ 35''$, respectively. The strongest of these sources was useful as a control source to check the flux density variations of CF Tuc and to give estimates of random errors. Fig. 4 shows the restored image of CF Tuc at 3.6 cm. This map also shows an unresolved point source with a peak flux level of 1.08 mJy beam^{-1}, with an angular size of < 0.7 arcsec. To aid in comparison, Figs 3 and 4 are plotted over approximately the same coordinate ranges and with the same contour levels as multiples of the rms noise in each image. The low-brightness extension to the south-west in Fig. 3 is not thought to be real.

The random error in the flux level was estimated by analysing the strongest confusing source in the 6-cm image plane. We found that the mean flux of this source over the entire data set was 1.26 mJy with an rms error of 0.12 mJy. Assuming this source has no intrinsic variation, an assumption that is partly justified by the dispersion, this then provides an estimate of the error in the CF Tuc fluxes. This can be compared with the 5σ level (0.20 mJy) in the subtracted map and with the mean error in the real component values (0.3 mJy). Based on the results of our error estimates, we believe that no flux variation less than about 16 per cent can be regarded as statistically significant.

4.2 Radio and EUV light curves

Figs 5(b) and (c) show the amplitude variation of the target against orbital phase for the 6-cm, 3.6-cm and EUV data. The orbital phase was calculated using the photometric ephemeris of Budding (1985) rather than that of Balona (1987) which is based on radial velocities. The estimated error in phase using this ephemeris is 0.0005. The radio flux density was formed as mentioned above by vector averaging after shifting to the phase centre. Also shown in Fig. 5(a) is the *V*-magnitude light curve of the system plotted with data from Budding & McLaughlin (1987). The fluxes at both radio frequencies vary consistently throughout the orbital phase and show their highest levels at about phase 0.5 (eclipse of the K4IV component). The EUV data shown in Fig. 5 have been binned to the same time resolution as the radio data over the 5 cycles of observations and been converted from count rate to flux. The increase that we see in the radio can be clearly seen in the EUV data over several days. To demonstrate that this feature is repeatable throughout the 5 cycles of EUV observations, we plot in Fig. 6(a) the EUV flux from each cycle against orbital phase. The enhancement centred at phase 0.5 clearly repeats consistently, and we believe therefore that this is a long-lived active region, rotational modulation or eclipsing behaviour and not a simple flare. However, it

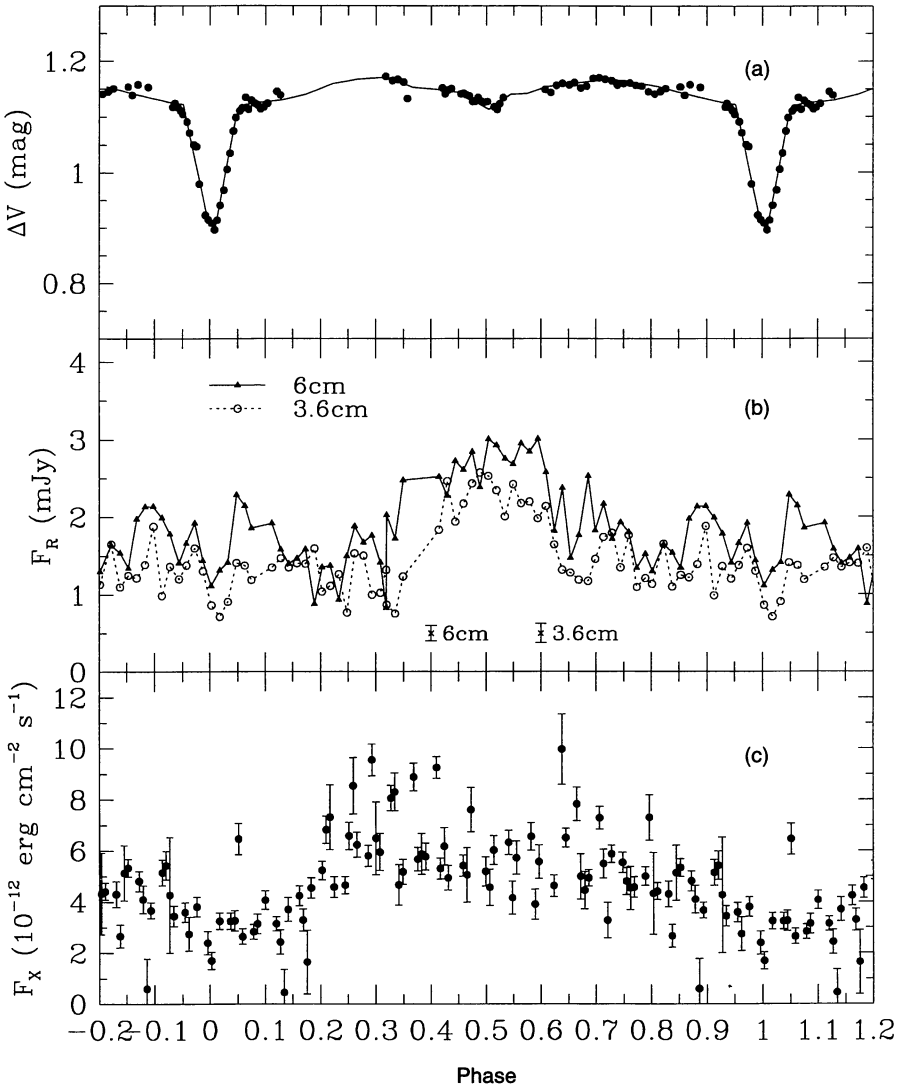

Figure 5. (a) The *V*-magnitude light curve of CF Tuc observed by Budding & McLaughlin (1987). (b) Time evolution of the 6- and 3.6-cm fluxes and (c) the EUV flux from CF Tuc, folded over the period and plotted against orbital phase. Also plotted are estimated error bars for the radio data. Data have been binned with the same temporal resolution.

should be noted that Kürster (1994) and Kürster & Schmitt (1996) have reported a very large flare-type outburst from CF Tuc in 1992 October/November observed in the *ROSAT* 0.1–2.4 keV band, which released 4.5×10^{36} erg over a nine-day interval.

From our analysis we conclude that both stars in the CF Tuc system are active coronal emitters in the radio and EUV regions. The minima in the radio and EUV light curves occur when the smaller G star is partially occulted by the larger K4 subgiant, as can be seen in Fig. 5(a). This could be explained by associating active regions with the G star, and this interpretation of the EUV data has been suggested by Schmitt et al. (1996). However, we wish to investigate the other possibility that the active regions are associated with the K-star hemisphere facing the G star. This is primarily because the activity in CF Tuc is normally attributed to the subgiant component (Cameron et al. 1981; Coates et al. 1983), as is common for RS CVn binaries. Using a large sample of solar neighbourhood stars, Mathioudakis et al. (1995) have presented an activity versus rotation relation in the EUV. If we assume that most of the EUV flux arises from the G0V companion, a comparison with the results of Mathioudakis et al. (1995) would place the G0V star amongst the most active dwarfs with the same rotational period. The possibility that the G star may be the primary source of the coronal emission cannot therefore be excluded.

Our observations show a fairly smoothly varying increase in radio and EUV flux in the phase range 0.4–0.7. We immediately draw attention to the comprehensive analysis of over 16 years of photometric observations recently presented by Budding & Zeilik (1995). These authors saw clear evidence for preferred longitudes for the formation of maculation on the surface of the K star in CF Tuc. Although the longitudinal formation of spots seemed to vary with a period of 5–6 yr, the preferred longitude occurred close to but a little before the phase of primary minimum (phase 1.0). This is quite the opposite to what we see in the radio and EUV. However, independent photometry of CF Tuc obtained by Rounthwaite (private communication) in 1994, and covering the period of our observations, indicates a consistent maculation-type depression centred on the same phase range of 0.4–0.7. More recently, Budding et al. (1996) re-observed CF Tuc with the ATCA at four

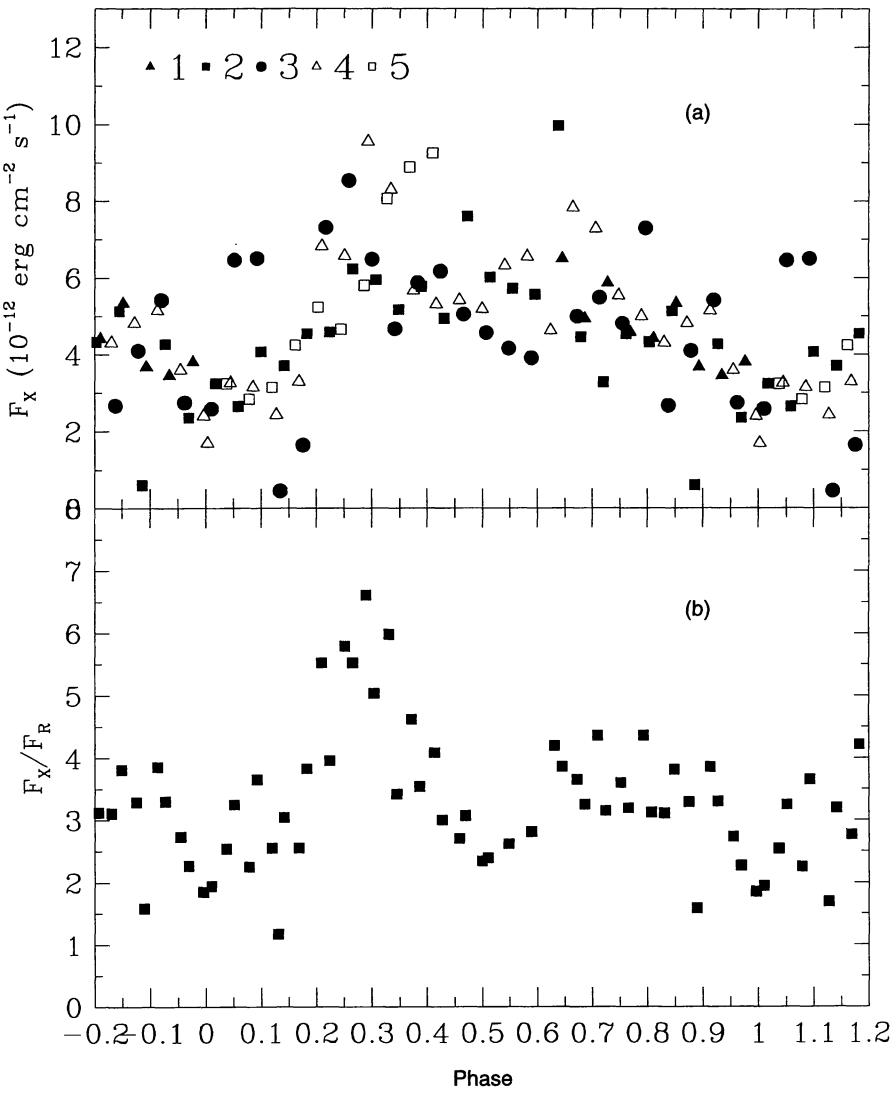

Figure 6. (a) The individual cycle observations (5 cycles) of EUV flux from CF Tuc. (b) Time evolution of the EUV flux divided by the 6-cm flux (F_X/F_R in arbitrary units) from CF Tuc plotted against orbital phase.

frequencies, and their preliminary radio light curves again show a general increase in flux at phase 0.4–0.7.

We therefore assume that the feature seen in our data is a very long-lived feature of enhanced radio and EUV emission situated in the intra-binary region and probably associated with active regions on the facing surface of the K4 subgiant. The question of whether the EUV and radio emission regions are cospatial should be addressed. As we point out in Section 4.5, the apparent quadrature maxima in the EUV light curve imply an intra-binary origin. However, the EUV variations may be consistent with separate coronae associated with each star in the system. Thus the emitting volumes of the thermal and non-thermal electrons need not be cospatial but could be much different in size. Cospatiality has not been tested observationally. However, X-ray observations of active stars often imply a two-temperature corona (Swank et al. 1981). The hot X-ray component is more frequently correlated with steady microwave emission (Drake et al. 1989) and generally does not show eclipses (Culhane et al. 1990; White et al. 1987), implying that these components are extended regions of several stellar radii. White, Lim & Kundu (1994) also concluded that the hot X-ray plasma was not coincident with strong magnetic fields in the lower corona. Furthermore, the lifetime of an MeV electron in the cooler plasma component is short enough that the steady radio emission would require almost continuous particle injection, implying that the radio-emitting electrons also reside in extended regions. This is confirmed by high-resolution VLBI observations (e.g. Mutel et al. 1985). Hence the radio/X-ray correlation suggests the possibility of cospatiality, although it is possible that the correlation arises simply because the same process that accelerates the relativistic particles also heats the corona. Franciosini & Chiuderi Drago (1995) presented a magnetic loop model for an RS CVn star in which non-thermal particles are injected in the local thermal plasma. The derived emission characteristics, source structure and evolution were found to be in general agreement with observations. Also the emission measure compared well with those derived from X-ray observations, which allows for cospatiality. We thus assume in the following discussion that the X-ray and radio emission regions are cospatial, but this assertion would benefit from further observations.

4.3 Characteristics of the radio emission

In this section we derive some characteristics of the radio emission under the assumption that it is due to gyrosynchrotron emission from mildly relativistic electrons. We would, however, refer the reader to our discussion in Section 4.4. In order to calculate the brightness temperature of the radio emission from CF Tuc, an estimate of the angular extent of the source is required. Owing to the nature of the light curve, we take the maximum source size to be equal to the separation of the binary system (2×10^{11} cm). An upper limit to T_b at 6 cm is given by

$$T_b = 7.1 \times 10^7 S_6/\theta^2, \quad (1)$$

where S_6 is the mean observed 6-cm flux density measured in mJy and θ is the source angular dimension in milliarcseconds. The lower limit to T_b is then 2.2×10^8 K which is consistent with the 6-cm brightness temperatures on some active stars (Lang 1990).

The dual-frequency observations of CF Tuc at 4.8 and 8.64 GHz have revealed mean fluxes of $\sim$1.9 and $\sim$1.1 mJy respectively, which give a spectral index of ~ -1.0. This implies that a non-thermal population is responsible for the emission, or that $\nu_{peak} \sim \nu_{observed}$ and the source is becoming optically thin at these frequencies. The brightness temperature for optically thin radiation depends on the magnetic field strength, the observing frequency and the electron energy spectral index δ which is unknown. In reality, then, $T_b \sim \tau T_{eff}$ where τ is the optical depth and T_{eff} is the effective temperature of the electrons. Assuming for simplicity that the emission is still optically thick at 6 cm ($\tau \sim 1$), then the energy of the emitting electrons is given by

$$E_{eff} = 8.6 \times 10^{-10} T_{eff} \text{ MeV}, \quad (2)$$

which with $T_b \sim 2.2 \times 10^8$ K is 0.19 MeV. According to the results of Dulk (1985) this is possible (assuming $\delta \leq 3$) for all $\nu \geq 10\nu_B$ where ν is the observing frequency and ν_B is the plasma gyromagnetic frequency. This constraint implies that the magnetic field $B \leq 178$ G, since

$$B = \frac{\nu}{2.8s} \text{ G}, \quad (3)$$

where $s = \nu/\nu_B$ and ν is in MHz. Assuming for the moment that the secondary component in CF Tuc is the source of a dipole magnetic field given by

$$B = B_0 \left(\frac{R}{R_\star}\right)^{-3}, \quad (4)$$

where B_0 is the surface induction, $R_\star$ is the stellar radius and R is the radial position of the $\tau \sim 1$ surface (assumed to be the binary separation), then the surface field is $B_0 \sim$ 1140 G. These calculations are only suggestive, since they assume not only that $\tau \sim 1$ but also that the field is dipolar. However, if the emission peak frequency lies in the range 1–15 GHz, the derived magnetic fields do not vary by more than a factor of 0.3–3.0.

It is also possible to infer the electron density in the emission region as follows. Again assuming an optically thick source and assuming gyrosynchrotron emission from mildly relativistic electrons with a power index of $\delta \sim 3$ then, following Dulk & Marsh (1982), the peak in the radio emission is given by

$$\nu_{peak} \approx 1.5 \times 10^4 (N_R L)^{0.23} B^{0.77}, \quad (5)$$

where a nominal viewing angle of $\theta = 45°$ is assumed, L is the length-scale of the emission region, B is the magnetic field and N_R is the relativistic electron density. Assuming $\nu_{peak} \sim \nu_{observed}$, $B \sim$ 178 G and L is equal to the maximum size of the emission region, then $N_R \sim 1.5 \times 10^5$ cm^{-3}. This value is somewhat smaller than that found in the extended emission regions around other RS CVn binaries (Mutel et al. 1984; Lestrade et al. 1988) but is consistent with the emission peak lying in the range 1–15 GHz. The above calculations show that, within the limits of the assumptions, the radio flux from CF Tuc is consistent with a large volume of plasma radiating by gyrosynchrotron emission from mildly relativistic electrons with inferred magnetic field strengths and electron densities comparable to those seen in other active binary stars. However, the assumption that $\tau \sim 1$ means that the derived emission characteristics are somewhat uncertain.

4.4 Electron populations

Soft X-ray observations of several classes of active stars have provided conclusive evidence for the presence of coronal material at temperatures of 10^7 K, although at least some of the most active systems possess a higher temperature component (Swank et al. 1981; Vaiana et al. 1981; Majer et al. 1986; Doyle, van den Oord & Kellett 1992). The curvature of the 0.5–10 keV spectrum for RS CVns and the presence of line complexes are strongly in favour of a thermal origin for these high-temperature components characteristic of solar flare plasma. Current understanding is that this hot material is confined and heated in closed coronal magnetic fields, as is seen in solar active regions.

The radio emission from RS CVn-type binaries generally appears to take three distinct forms. During *quiescent* emission the radiation is moderately circularly polarized with brightness temperatures of 10^{8-9} K, and has a nearly flat spectrum at centimetre wavelengths. More intense *flare* emission is characterized by unpolarized radiation with brightness temperatures $\geq 10^{10}$ K and a spectrum showing a positive spectral index. These flaring episodes typically last a few hours to days (Spangler, Owen & Hulse 1977). Occasionally high-intensity short-duration outbursts are seen displaying high degrees of circular polarization. These three phases of emission are normally attributed to gyrosynchrotron, synchrotron and electron cyclotron maser emission respectively. An important outcome of research in these two regimes is the apparent correlation between the radio and X-ray luminosities, L_R and L_X, in active stars. Drake et al. (1989) found a distinct relationship between L_R and L_X for active binaries, while, more recently, Güdel & Benz (1993) found $L_X \sim 10^{15.5 \pm 0.5} L_R$ valid over six orders of magnitude in both variables for all active late-type stars and solar flares. The existence of such a correlation is difficult to accept, given the differences in the assumed emission mechanisms and particle energy distributions. Since Drake et al. (1992) recently discussed this dilemma in depth, we refrain from a detailed discussion, but briefly review below the essential points of the controversy.

The L_R–L_X relationship could be easily understood if both emission processes were either thermal or non-thermal. The X-ray emission process is undoubtedly of a thermal nature. If the radio emission is gyrosynchrotron from a thermal population then observations suggest field strengths of 200 G in the emission region, which, assuming a dipolar field, requires surface magnetic fields of $\geq$ 3600 G. Such strong fields would be easily observable using Zeeman-broadening techniques, but as yet have not been found (Donati et al. 1990). More crucially the radio flux would be expected to fall as ν^{-8} beyond its peak frequency, but observations have shown only slow declines in flux with frequency (Chiuderi-Drago & Klein 1990; Massi & Chiuderi-Drago 1991). For these reasons a thermal population is thought unlikely to be the source of the radio emission. A non-thermal population of electrons in which

the energy distribution is characterized by a power-law spectral index δ also encounters difficulties when applied to the quiescent radio emission. This mechanism requires an almost continuous injection of non-thermal particles into the stellar corona. Apart from flares, the solar X-ray and microwave radiation can both be explained with thermal populations. However, the gross properties of active stars at centimetre wavelengths imply that the emission mechanism is non-coherent gyrosynchrotron emission from a non-thermal electron population. To date only tentative suggestions have been made concerning whether the relationship between thermal and non-thermal particles is *causal* or *common* (see Güdel & Benz 1993). A recent proposal was made by Linsky (1996) that the connection may lie in the acceleration of particles exceeding the thermal speed when the electric field in flares exceeds the Dreicer field. A detailed model linking thermal and non-thermal populations is yet to be developed.

It seems appropriate to address the problem of whether simultaneous radio and EUV observations can be used to disentangle the particle population question. We consider below the predicted ratio of radio to EUV luminosity for a cospatial plasma assuming (1) the same thermal population of electrons and (2) two unrelated populations, one thermal, and the other non-thermal, giving rise to the EUV and gyromagnetic radio emission respectively. We demonstrate that this ratio is inadequate for distinguishing the population type except for very extreme limits in the observational data. The conclusions of these calculations depend critically on our assumption of cospatiality. For the EUV radiation which is thermal (and assuming pure free–free radiation), the total emission is given by

$$L_X = 2.4\times10^{-27}T^{1/2}N_X^2V_X, \tag{6}$$

where V_X is the EUV source volume, L_X is in erg s^{-1} and we have assumed standard cosmic abundances and an index of refraction of unity. The total radio emission in erg s^{-1} Hz^{-1} can be written

$$L_R = \eta V_R, \tag{7}$$

where V_R is the radio source volume and η is the gyrosynchrotron emissivity. If the radio emission is from thermal electrons, then, using the results of Dulk (1985), we have

$$\eta \sim 6\times10^{-23}T^8\sin^6\theta B^{11}\nu^{-10}N_R\left(\frac{\nu}{\nu_B}\right)^2, \tag{8}$$

where ν_B is the electron gyrofrequency, B is the magnetic field strength and θ is the angle between the line of sight and the magnetic field. If we assume a power-law energy spectrum of non-thermal electrons that is isotropic in pitch angles [i.e. $n(E) = kE^{-\delta}$, where $2 \leq \delta \leq 7$] then the gyrosynchrotron emissivity is

$$\eta = 3.3\times10^{-24}10^{-0.52\delta}(\sin\theta)^{-0.43+0.65\delta} \times\left(\frac{\nu}{\nu_B}\right)^{1.22-0.90\delta}BN_R. \tag{9}$$

We now assume $\delta \sim 3$ and that the emission is cospatial by writing $V_X \sim V_R$. The ratios of radio to EUV luminosities for the thermal and non-thermal cases, R_t and R_{nt} respectively, are then

$$R_t = 2.5\times10^4T^{7.5}\sin^6\theta B^{11}\nu^{-10}N_RN_X^{-2}\left(\frac{\nu}{\nu_B}\right)^2\text{Hz}^{-1}, \tag{10}$$

$$R_{nt} = 37.87T^{-\frac{1}{2}}(\sin\theta)^{1.52}BN_RN_X^{-2}\left(\frac{\nu}{\nu_B}\right)^{-1.48}\text{Hz}^{-1}. \tag{11}$$

Assuming that the viewing angle is $\theta = 90°$, corresponding to the maximum in gyrosynchrotron flux, we can now calculate limits to R_t and R_{nt} as a function of ν/ν_B using appropriate ranges of the dependent variables. We take the values $B \sim 10$–200 G, $\nu/\nu_B \sim 10$–100, $N_R \sim 10^6$–10^8 cm^{-3}, $N_X \sim 10^{10}$–10^{12} cm^{-3} and $T \sim 10^6$–10^8 K. In Fig. 7 we plot the maximum and minimum values of $\log R$ against ν/ν_B for the thermal and non-thermal cases using these ranges of variables. The minimum R_t curve is not depicted since it lies at approximately $\log R = -55.0$. Fig. 7 displays immediately that, given the expected range of parameters for the emission processes, we cannot determine if the electron population is thermal or non-thermal from EUV and radio fluxes. The range of R for a non-thermal population only barely exceeds the range of R for a thermal population because the latter is more strongly dependent on the field strength and temperature.

There are a number of developments required in order to settle the debate over the link between radio and X-ray emission in active stars. In the radio the exact location of the peak frequency in the spectrum and the slopes of the continua either side of this peak are required. Although some radio spectral investigations have been performed (Güdel 1994; Chiuderi Drago & Franciosini 1993) and imply a non-thermal population, this is an area which requires more observational work. Information on the circular polarization would also be helpful in determining the electron population since, if the emission is known to be optically thick, a thermal electron population predicts zero polarization, while for the non-thermal case it would be of the order of ≤ 10 per cent (Dulk 1985). If the emission is optically thin then both thermal and non-thermal populations can give rise to high polarizations of ≤ 50 per cent. We have demonstrated that simultaneous EUV observations are not sufficient to constrain the details of the process. We are therefore unable to refine our estimates of the physical parameters given in Section 4.3. Until a detailed model of the electron acceleration process is developed and observations are performed specifically to determine the form of the gyrosynchrotron electron population, this question must remain unanswered.

In Fig. 7 we have plotted the empirical ratio of radio to X-ray luminosity for active single and binary stars of spectral types F to M given by Güdel & Benz (1993). This correlation ($\log L_R/L_X \sim -15.5$) was found to be valid over six orders of magnitude for both quantities. Unfortunately this ratio is found to lie just where the two populations become ambiguous for this set of parameters, and therefore it is impossible to determine the population without independent values for densities, magnetic fields and temperatures. However, the tightness of the relationship (see Güdel 1994) immediately constrains the range of parameters allowed in each case. The scatter in the observed relationship may imply that thermal electrons are not responsible for the radio emission because of the extreme dependence on magnetic field. An inherent relation between B and energy distribution may therefore be appropriate. Our 6-cm observational ratio of -14.2 for CF Tuc (corrected for the line-to-continuum ratio) is found to be significantly greater than the observed ratio, although it should be pointed out that the DS passband is different from both the *ROSAT* and *Einstein* passbands. Using the *ROSAT* All Sky Survey X-ray flux of $L_X = 3.45\times10^{30}$ erg s^{-1} given by Dempsey et al. (1993), the $\log L_R/L_X$ value is -14.5. Hence CF Tuc appears to be either under-luminous in the EUV or over-luminous in the radio (or both) compared with other active stars. The high radio flux values imply that the radio emission may be higher than expected on the basis of the correlation observed by Güdel & Benz (1993). It should be noted that Güdel & Benz (1993) do not suggest that the same population of electrons produces both the radio and X-ray emission, but that the mechanism which accelerates the electrons also heats the corona. As stated previously, the above conclusions depend critically on our assumption of cospatiality.

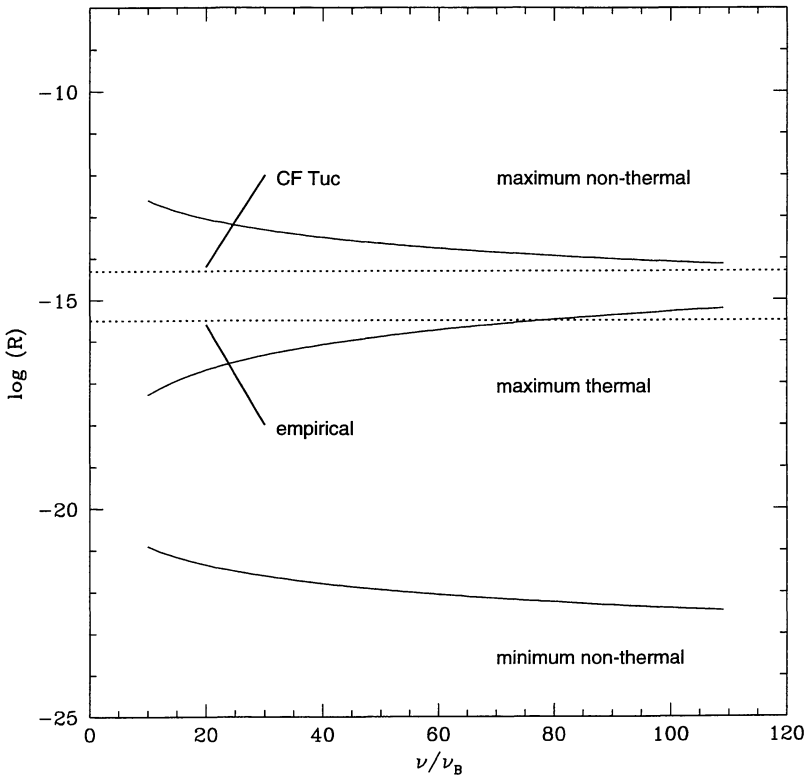

Figure 7. Variation of the ratio R of radio to EUV luminosity with ν/ν_B for assumed ranges of the emission parameters. The upper curve shows the maximum attainable ratio if the gyrosynchrotron electron population is non-thermal; the lowest curve shows the minimum in R for this population. The dotted lines show the empirically derived ratio for active stars of all types (Güdel & Benz 1993) and the ratio observed for CF Tuc.

4.5 Directivity

Using the orbital and stellar parameters for CF Tuc, it is easy to calculate that at secondary conjunction (phase 0.5) approximately 25 per cent of the K4IV star's surface is obscured. At primary conjunction when the hotter star is eclipsed, almost all of its surface is obscured by the larger component. If the EUV emission originated in an isotropically radiating thermal plasma in the intra-binary region, we would therefore expect to observe maximum flux at quadratures, minimum at primary conjunction and intermediate values at secondary conjunction. The EUV light curve appears to show such a variation, but the radio light curve does not. This difference is emphasized in Fig. 6(b) where we plot the EUV-to-radio flux ratio in arbitrary units, and which shows obvious enhancement of flux at phase 0.25, possible enhancement at phase 0.75 and minima elsewhere. We believe that this difference arises because the gyrosynchrotron emission displays intrinsic directivity caused by preferential emission about a broad maximum peaked in the direction of instantaneous motion of the accelerated electrons. Lim et al. (1994) recently discussed the possible physical conditions that can give rise to directivity of radio emission. They analysed ATCA observations of AB Dor and considered absorption and ducting by coronal material and intrinsic directivity. They concluded that gyro-emission from ultrarelativistic electrons within a magnetic loop could account for the observed radio flux modulation. The possibility of intrinsic directivity of radio emission from stellar objects has hitherto been ignored in most studies.

Radiation from an ensemble of relativistic electrons (with Lorentz factor γ) gyrating in a magnetic field is beamed into a cone in a direction along the particle's instantaneous motion of half-angle $\phi \sim 1/\gamma$. For mildly relativistic electrons (gyrosynchrotron emission), $\gamma \sim 2$–3 and the width of this cone would be $\theta \geq 38°$. The radio flux would display a maximum when the magnetic field is perpendicular to the observer's line of sight. This model requires the presence of highly energetic particles which would have short lifetimes before being precipitated into the stellar chromosphere. However, as pointed out by Lim et al. (1994), a population of *trapped* electrons can still be responsible for the emission, provided only that there is a narrow distribution of large pitch angles and that interactions with plasma waves (Kundu et al. 1987) do not scatter these particles to smaller pitch angles. The former requirement is satisfied if the magnetic field does not diverge too rapidly with height. With a magnetic loop structure where electrons are trapped at the loop apex, the gyrosynchrotron emission will have directivity if the line joining the footpoints of the loop has a component in the equatorial plane of the stellar source. The details of such a model require refinement since the shape of the $\tau \sim 1$ emission surface in various field configurations has not been investigated, although Stewart et al. (1988) provided a simple model of a dipolar field. Nevertheless, the $\sin\theta$ dependence is likely to dominate the emission characteristics even in quite distorted loop apexes. In summary, we believe that a possible explanation for the radio modulation is that we have observed intrinsic directivity of the gyrosynchrotron emission. Without further observational work this conclusion must remain tentative.

4.6 Intra-binary emission in active binaries

There has been much debate concerning the origin of the large-scale coronal structures in RS CVn binaries and the importance of

binarity for their formation. It has been proposed that a single magnetic dipole centred on the active star may be responsible for this emission. On the basis of X-ray observations (Walter et al. 1980; Swank et al. 1981) it appears that there must exist large coronal loops in active binary systems in order to constrain the hot corona. These must be comparable in size to the binary separation. VLBI observations (Mutel et al. 1985) have also indicated that radio coronae are large in comparison with the stellar radius.

Mutel et al. (1985) suggested a time-dependent model of the emission to account for the observed properties of RS CVn systems in the radio. In this model, electrons are accelerated in a compact region which expands outwards while the electrons lose their energy by synchrotron radiation. Eventually the source expands enough to become optically thin and appears as an extended halo. This model also explains how it is possible to have large extended structures without the compact source, since the core will fade by radiative losses in a short time-scale while the halo fades more slowly because of the weaker magnetic field. In the core–halo model, large negative values of α can occur when the emission is dominated by the optically thin halo with small power-law indices of $\delta \leq 3$. However, small values of δ imply more highly energetic electrons, which should be expected during flares rather than quiescent periods (Morris, Mutel & Su 1990). However, as pointed out by Mutel et al. (1987), the flat or inverted spectrum may be indicative of emission from a number of different source regions with different physical characteristics. This has been demonstrated in recent observations of UX Ari by Chiuderi-Drago & Franciosini (1993), who showed that a flat spectrum can persist for many days after a flare. Mutel et al. (1987) suggested that the spectral index of the emission from RS CVn systems was correlated with the luminosity. As shown by Franciosini & Chiuderi Drago (1995), this can be interpreted as the evolution of the emission source from an intense optically thick flare-related region to a less intense optically thin halo-type structure.

Another possibility for the large coronae of active close binaries is that a joint magnetosphere exists between the two stars. This is possible since both are likely to have deep convective envelopes necessary to drive the magnetic dynamo. This mechanism was proposed by Uchida & Sakurai (1983) and Uchida (1986), who suggested that the existence of stellar differential rotation in the radial direction can lead to twisting of magnetic flux tubes and the subsequent release of energy during reconnection of loops with scales comparable to the size of the binary system. Doyle, van den Oord & Byrne (1989) suggested an intra-binary connection as a means of explaining the very large flare energy requirements in these objects. Furthermore, Simon, Linsky & Schiffer (1980) also suggested a scenario of interacting magnetic flux tubes to account for the UV properties of UX Ari. Recent VLBI astrometric results by Lestrade (1996) clearly showed that in the two RS CVn systems UX Ari and σ^2 CrB the preferred site of quiescent radio emission is in the intra-binary region. Lestrade (1996) suggests that interactions in this region between magnetic loops from both stars might produce the required electron acceleration. The problems with this theory are that some single active stars have been shown to display very similar features to the RS CVn binaries (Turner 1985; Morris & Mutel 1988), and some dependence of polarization on orbital phase would be expected if the fields were simple.

One important result that is now universally accepted is that the active close binaries appear to be more active in the radio regime than single stars with similar properties (Gibson 1980). In this respect the binarity of these systems is an important factor in the generation of the magnetic activity. In our research programme we have attempted to use the radio eclipse-imaging technique to derive details on the environments of active close binaries. A comparison of the radio properties of RS CVn systems and Algols provides viable tests of the interacting field and core–halo expansion models. We have found that the CF Tuc system shows evidence of enhanced radio and EUV emission at 0.5 orbital phase, although the overall extent of the corona is large. The form of the light curves suggests that this emission is in fact originating in the intra-binary region and may therefore be a consequence of binarity. In a subsequent paper (Gunn et al., in preparation) we will present evidence of a similar intra-binary region in the Algol system V505 Sgr. These results complement those of Lestrade (1996) and imply that field interaction may be important in the formation of the coronae of active close binary stars. It is possible that the core–halo structures seen in such systems can be associated with activity in the intra-binary region, although this assertion requires a great deal of additional observational and theoretical work before being confirmed.

5 CONCLUSIONS

We have analysed 6- and 3.6-cm synthesis observations of the active RS CVn-type binary CF Tuc in order to investigate the existence of phase-related eclipses of the radio corona. We have also analysed contemporaneous EUV data from the *EUVE* Deep Survey/Spectrometer telescope. In the 6-cm, 3.6-cm and EUV data there is evidence of enhanced emission from CF Tuc at an orbital phase of 0.5. The form of the light curves suggests that the increased emission is associated with an intra-binary region and that the gyrosynchrotron emission displays intrinsic directivity associated with energetic electrons trapped in the apex of a coronal loop. The existence of an intra-binary region of emission has serious implications for the details of field interaction and coronal formation in active close binary stars. We have demonstrated that simultaneous observations in the EUV and radio are not sufficient to determine the characteristics of the gyrosynchrotron electron population. The existence of a tight relationship between X-ray and radio luminosity immediately constrains the range of allowed parameters for the emission.

ACKNOWLEDGMENTS

Research at Armagh Observatory is grant aided by the Department of Education for Northern Ireland. We also acknowledge computer support by the Starlink project funded by the UK PPARC. MM thanks the *EUVE* principal investigators Drs S. Bowyer and R. F. Malina for their advice and support. This work has been supported in part by a Royal Society grant to Queen's University of Belfast. AGG thanks Armagh Observatory for a research scholarship during the period of this work. Acknowledgments also go to the ATNF director and staff (in both Epping and Narrabri), to Bob Sault, Neil Killeen and Haida Liang for a worthy introduction to the MIRIAD software. This work was supported by PPARC Grant No. GR/K34993. The authors also thank the referee (J. L. Linsky) for suggestions on how to improve this paper.

REFERENCES

Balona L. A., 1987, S. Afr. Astron. Obs., Circ., 11, 1
Bowyer S., Lieu R., Lampton M., Lewis J., Wu X., Drake J. J., Malina R. F., 1994, ApJS, 93, 569
Brown R. L., Broderick J. J., Neff S. G., 1979, BAAS, 4, 630
Budding E., 1985, Inf. Bull. Variable Stars, No. 2779

Budding E., McLaughlin E., 1987, Ap&SS, 133, 45
Budding E., Zeilik M., 1995, Ap&SS, 232, 355
Budding E., Allen D., Crawford D. L., Jones K. M., Slee O. B., Zeilik M., 1996, in Lee H. M., Kim S. S., eds, Proc. 7th Asian Pacific Regional Meeting of the IAU, in press
Cameron A. C., Hearnshaw J. B., Austin R. R. D., 1981, MNRAS, 197, 769
Chiuderi-Drago F., Franciosini E., 1993, ApJ, 410, 301
Chiuderi-Drago F., Klein K.-L., 1990, Ap&SS, 170, 81
Coates D. W., Halprin L., Sartori P. A., Thompson K., 1983, MNRAS, 202, 427
Collier A. C., Hearnshaw J. B., Austin R. R. D., 1981, MNRAS, 197, 769
Collier A. C., Haynes R. F., Slee O. B., Wright A. E., Hillier D. J., 1982, MNRAS, 200, 869
Culhane J. L., White N. E., Shafer R. A., Parmar A. N., 1990, MNRAS, 243, 424
Dempsey R. C., Linsky J. L., Fleming T. A., Schmitt J. H. M. M., 1993, ApJS, 86, 599
Doiron D. J., Mutel R. L., 1984, AJ, 89, 430
Donati J.-F., Semel M., Rees D. E., Taylor K., Robinson R. D., 1990, A&A, 232, L1
Doyle J. G., van den Oord G. H. J., Byrne P. B., 1989, A&A, 193, 229
Doyle J. G., van den Oord G. H. J., Kellett B. J., 1992, A&A, 262, 533
Drake S. A., Simon T., Linsky J. L., 1989, ApJS, 71, 905
Drake S. A., Simon T., Linsky J. L., 1992, ApJS, 82, 311
Dulk G. A., 1985, ARA&A, 23, 169
Dulk G. A., Marsh K. A., 1982, ApJ, 259, 350
Franciosini E., Chiuderi Drago F., 1995, A&A, 297, 535
Gibson D. M., 1980, in Plavec M. J., Ulrich R. K., eds, Proc. IAU Symp. 88, Close Binary Stars: Observations and Interpretation. Reidel, Dordrecht, p.31
Güdel M., 1994, ApJS, 90, 743
Güdel M., Benz A. O., 1993, ApJ, 405, L63
Gunn A. G., 1996, Irish Astron. J., 23, 33
Gunn A. G., Migenes V., Doyle J. G., Spencer R. E., 1996, in Taylor A. R., Paredes J. M., eds, ASP Conf. Ser. Vol. 93, Radio Emission from the Stars and the Sun. Astron. Soc. Pac., San Francisco, p. 321
Kundu M. R., Jackson P. D., White S. M., Melozzi M., 1987, ApJ, 312, 822
Kürster M., 1994, in Caillault J.-P., ed., Proc. 8th Cambridge Workshop, ASP Conf. Ser. Vol. 64, Cool Stars, Stellar Systems and the Sun. Astron. Soc. Pac., San Francisco, p. 104
Kürster M., Schmitt J. H. M. M., 1996, A&A, 311, 211
Lang K. R., 1990, in Mirzoyan L. V., Pettersen B. R., Tsvetkov M. K., eds, Proc. IAU Symp. 137, Flare Stars in Star Clusters, Associations and the Solar Vicinity. Kluwer, Dordrecht, p. 125
Lestrade J. F., 1996, in Strassmeier K. G., Linsky J. L., eds, Proc. IAU Symp. 176, Stellar Surface Structure. Kluwer, Dordrecht, p. 173
Lestrade J. F., Mutel R. L., Preston R. A., Phillips R. B., 1988, ApJ, 328, 232
Lim J., White S. M., Nelson G. J., Benz A. O., 1994, ApJ, 430, 332
Linsky J. L., 1996, in Taylor A. R., Paredes J. M., eds, ASP Conf. Ser. Vol. 93, Radio Emission from the Stars and the Sun. Astron. Soc. Pac., San Francisco, p. 439
Majer P., Schmitt J. H. M. M., Golub L., Harnden F. R., Rosner R., 1986, ApJ, 300, 360
Malina R. F. et al., 1994, AJ, 107, 751
Manchester R. N., 1991, Adv. Space Res., 11, 403
Massi M., Chiuderi-Drago F., 1991, A&A, 253, 403
Mathioudakis M., Fruscione A., Drake J. J., McDonald K., Bowyer S., Malina R. F., 1995, A&A, 300, 775
Mewe R., Gronenschild E. H. B. M., van den Oord G. H. J., 1985, A&AS, 62, 197
Miller A., Abbott M., 1995, *EUVE* Guest Observer Software User's Guide, Version 1.5
Mitrou C. K., Mathioudakis M., Doyle J. G., Antonopoulou E., 1997, A&A, 317, 776
Morris D. H., Mutel R. L., 1988, AJ, 95, 204
Morris D. H., Mutel R. L., Su B., 1990, ApJ, 362, 299
Mutel R. L., Doiron D. J., Lestrade J. F., Phillips R. B., 1984, ApJ, 278, 220
Mutel R. L., Lestrade J. F., Preston R. A., Phillips R. B., 1985, ApJ, 289, 262
Mutel R. J., Morris D. H., Doiron D. J., Lestrade J. F., 1987, AJ, 93, 1220
Owen F. N., Gibson D. M., 1978, AJ, 83, 1488
Rucinski S. M., 1983, Inf. Bull. Variable Stars, No. 2270
Rumph T., Bowyer S., Vennes S., 1994, AJ, 107, 2108
Schmitt J. H. M. M., Stern R. A., Drake J. J., Kürster M., 1996, ApJ, 464, 898
Simon T., Linsky J. L., Schiffer F. H., 1980, ApJ, 239, 911
Slee O. B., Nelson G. J., Stewart R. T., Wright A. E., Innis J. L., Ryan S. G., Vaughan A. E., 1987, MNRAS, 229, 659
Spangler S. R., Owen F. N., Hulse R. A., 1977, ApJ, 82, 989
Stewart R. T., Innis J. L., Slee O. B., Nelson G. J., Wright A. E., 1988, AJ, 96, 371
Swank J. H., Holt S. S., White N. E., Becker R. H., 1981, ApJ, 246, 208
Turner K. C., 1985, in Hjellming R. M., Gibson D. M., eds, Radio Stars. Reidel, Dordrecht, p. 283
Uchida Y., 1986, Highlights Astron., 7, 461
Uchida Y., Sakurai T., 1983, in Rodono M., Byrne P. B., eds, Proc. IAU Colloq. 71, Activity in Red Dwarf Stars. Reidel, Dordrecht, p. 629
Umana G., Trigilio C., Hjellming R. M., Catalano S., Rodono M., 1993, A&A, 267, 126
Vaiana G. S. et al., 1981, ApJ, 245, 163
Walter F. M., Bowyer S., 1981, ApJ, 245, 671
Walter F. M., Cash W., Charles P. A., Bowyer C. S., 1980, ApJ, 236, 212
White N. E., Culhane J. L., Parmar A. N., Sweeney M. A., 1987, MNRAS, 227, 545
White S. M., Lim J., Kundu M. R., 1994, ApJ, 422, 293

This paper has been typeset from a TEX/LATEX file prepared by the author.